

**N 9 4 - 1 1 4 0 1**

## **SPACE STATION FREEDOM ADVANCED PHOTOVOLTAICS AND BATTERY TECHNOLOGY DEVELOPMENT PLANNING<sup>1</sup>**

Spruce M. Cox, Boeing Defense & Space Group, Huntsville, AL 35824  
Mark T. Gates, Scott A. Verzwylt, Boeing Defense & Space Group, Seattle, WA 98124  
Karen D. Brender, NASA Langley Research Center, Hampton, VA 23665

### **1.0 Introduction**

Space Station Freedom (SSF) usable electrical power is planned to be built up incrementally during assembly phase to a peak of 75 kW end-of-life (EOL) shortly after Permanently Manned Capability (PMC) is achieved in 1999. This power will be provided by planar silicon (Si) arrays and nickel-hydrogen (NiH<sub>2</sub>) batteries. The need for power is expected to grow from 75 kW to as much as 150 kW EOL during the evolutionary phase of SSF, with initial increases beginning as early as 2002. Providing this additional power with current technology may not be as cost effective as using advanced technology arrays and batteries expected to develop prior to this evolutionary phase. A six-month study sponsored by NASA Langley Research Center and conducted by Boeing Defense and Space Group was initiated in August, 1991 (ref. 1). The purpose of the study was to prepare technology development plans for cost effective advanced photovoltaic (PV) and battery technologies with application to SSF growth, SSF upgrade after its arrays and batteries reach the end of their design lives, and other low Earth orbit (LEO) platforms. Study scope was limited to information available in the literature, informal industry contacts, and key representatives from NASA and Boeing involved in PV and battery research and development. The authors wish to thank all study contributors.

Ten battery and 32 PV technologies were examined and their performance estimated for SSF application. Promising technologies were identified based on performance and development risk. Rough order of magnitude cost estimates were prepared for development, fabrication, launch, and operation. Roadmaps were generated describing key issues and development paths for maturing these technologies with focus on SSF application.

### **2.0 Technology Goals**

SSF Si arrays and NiH<sub>2</sub> batteries were defined as the state-of-the-art (SOA) for this study. The technology goal for advanced PV was to double areal performance of the SOA arrays, from a blanket-level value of 95 W/sq m to 190 W/sq m or greater, while maintaining a 15 year design life. The battery technology goal was a 50% increase in operational specific energy of the SOA batteries, from 16 Whr/kg to 24 Whr/kg (cell level) or greater while maintaining a five year design life. Operational Whr/kg is defined as the nameplate Whr/kg rating of a battery multiplied by the depth of discharge (DoD), a more representative measure of merit than the nameplate rating alone. In both cases, the first increment of increased capability was to be available around the time of the first envisioned SSF growth increment, approximately 2002. This date was not a hard requirement. It was used to identify technologies that would mature approximately in time to support SSF growth.

### **3.0 Advanced Batteries**

#### **3.1 Technology Readiness Assessment**

Table I summarizes the technology readiness assessment of the 10 battery systems evaluated in this study. Readiness and risk values are estimated from standard definitions (readiness levels 1 [basic principles observed] to 7 [engineering model tested in space] and risk levels 10 [unknown materials/processes] to 1 [off-the-shelf]). Readiness levels were estimated based on the probability of a battery system demonstrating the study performance goal by the year 1996. This 1996 date would allow five years (battery design life used in this study) of real time battery/mission relevant testing prior to flight to confirm capability.

<sup>1</sup> This work was sponsored by the NASA Langley Research Center under contract #NAS1-19247.

Table I - Advanced Battery Technology Assessment

System Concept	Cell Performance [Whr/kg, oper Whr/kg*, Whr/liter]	Readiness Level	Risk Level
<b>SOA</b>			
• NiH2-Large IPV (HST)	45, 5, 70	7	2
• NiH2-Larger IPV (SSF)	46, 16, 74	6	4
<b>Advanced</b>			
• NiH2-Improved Mgmt**	48, 24, 74	5	4
• NiH2-Largest IPV	55, ?, 80	5	4
• NiH2-CPV	60, ?, 70	5	6
• NiH2-Bipolar/ CPV	75, ?, ?	4	7
• NiMH	45, 15, 160	5	5
• NaS-Tubular Electrolyte	110, 33, ?	4	7
• NaMCl2	140, ?, ?	3	8
• NaS-Thin Flat Electrolyte	220, ?, ?	3	8
* Operational Whr/kg---Nominal cell Whr/kg times depth of discharge (normalized to 30,000 cycles) ** Improved battery management/component to increase average depth of discharge vs life cycle function NiH2---Nickel Hydrogen, NiMH---Nickel Metal Hydride, NaS---Sodium Sulfur, NaMCl2---Sodium Metal Chloride, IPV---Individual pressure vessel, CPV---Common pressure vessel			

Prediction of cell level operational specific energy to obtain 30,000 LEO cycles (five year life) was central to this assessment. Operational specific energy was determined by derating the cell nameplate by the percent DoD that would achieve 30,000 cycles. At least five years of calendar life and the capability of high temperature systems to meet freeze/thaw requirements were assumed. Cell level specific energies were readily available in the literature, but DoD versus cycle life functions for most of these advanced systems were not. The baseline SSF NiH2 system was projected to support 35% DoD at 30,000 cycles by data available in the literature, but verification cell testing is currently only at the two-thirds point (ref. 2). Air Force qualification of NiH2 individual pressure vessel (IPV) for LEO is also short of the five year point (ref. 3). Extrapolation of performance data between NiH2 cell designs (for example IPV to common pressure vessel-CPV) was not attempted because of interaction of battery system operating parameters including LEO charge/discharge rates, electrolyte management, and thermal cycles.

### 3.2 Screening Results

The central screening criteria of candidate battery systems was its capability to meet or exceed the technology goal when the technology was incorporated into a flight system. Battery producibility must have been demonstrated. The system also had to have single point failure tolerance (cell short and open circuit).

A key screening analysis parameter was the DoD value that enabled a five year design life. There is sufficient evidence to suggest that the inherent DoD versus cycle life function of NiH2 IPV systems could be significantly improved (ref. 4,5). The Improved NiH2 IPV battery incorporated improvements in cell components and battery management to realize a DoD of 50%. Low development risk and minimal design impact on the baseline SSF system made the Improved NiH2 IPV a viable candidate. Modifications of the Improved NiH2 battery could be embodied in more advanced packaging designs. However, name plate specific energy gains attained through improved packaging of CPVs or larger IPV designs may not be realized operationally. Thermal path length at LEO charge/discharge rates and electrolyte and oxygen management issues may negate minor weight advantages by reduction of the DoD versus cycle life function.

Nickel metal hydride (NiMH) offers significant energy density improvement over the baseline NiH2. Effects of long term LEO cycling on metal hydride alloys need to be established, but reported results are encouraging (ref. 6). A cycle life improvement over NiH2 IPV is not anticipated. NiMH was evaluated at 30% DoD for a five year mission life.

Sodium sulfur (NaS) with tubular electrolyte is the most technically ready of the high temperature systems and offers significant improvement in name plate specific energy over the rechargeable nickel systems. Operational specific

energy prediction for the SSF application is difficult because of the very limited cycle life database. NaS with tubular electrolyte was evaluated at 30% DoD for a five year mission life.

### 3.3 Cost/Benefit Analysis

Relative costs that discriminated between technologies were estimated. These costs consist of technology development, hardware production, and launch. Calculations were performed at the battery level and did not include heat pipe/radiators, interconnects, and other structural elements associated with a battery ORU. Batteries were sized to provide the total SSF load during a 36 minute shadow at EOL. This would be a 45 kWhr load for a 75 kW station (90 kWhr for a 150 kW station). A 22% packaging weight penalty was applied to account for effects of integration of cells into batteries. A 10% spare cell count was included in the cost of production, but not for launch. A Space Shuttle launch cost factor of \$4620/kg was used (ref. 1). Table II summarizes DoD predicted to support a five year life in LEO, battery production costs based on name plate kWhr from reference 7 and data supplied by Eagle-Picher Industries, and ROM development costs of each system analyzed.

Table II - Battery Production Costs

System	DoD	\$K/kWhr	Develop Cost (\$M)
• SOA NiH2	35%	140	0
• Improved NiH2	50%	140	6

System	DoD	\$K/kWhr	Develop Cost (\$M)
• NiMH	30%	70	10
• NaS (Tubular)	30%	90	22

It was assumed that Improved NiH2 would be a refinement of the SOA NiH2, and hardware development costs were expected to be small. The NiMH development cost assumed that nickel cadmium (NiCd) and NiH2 cell components and integration elements are applicable. NiMH performance and its DoD versus cycle life function must be established. We assumed that the Air Force NaS tubular design has potential to achieve a 30,000 cycle life, but development costs would be high and must address major issues including consistency, DoD versus cycle life function, battery management/charge control, ORU structure, and thermal control materials and processes.

Cost/benefit analysis results are shown in Figures 1 and 2 for 75 kW and 150 kW battery complements, respectively. The 75 kW analysis applies to an increase in SSF capability from 75 kW to 150 kW. However, if the initial SSF battery complement is flown during initial SSF assembly planned for 1995-1996, its design life will be reached when the first complement of growth batteries are delivered around 2002. Replacement of the initial battery complement with new technology and addition of the growth batteries are included in the 150 kW analysis.

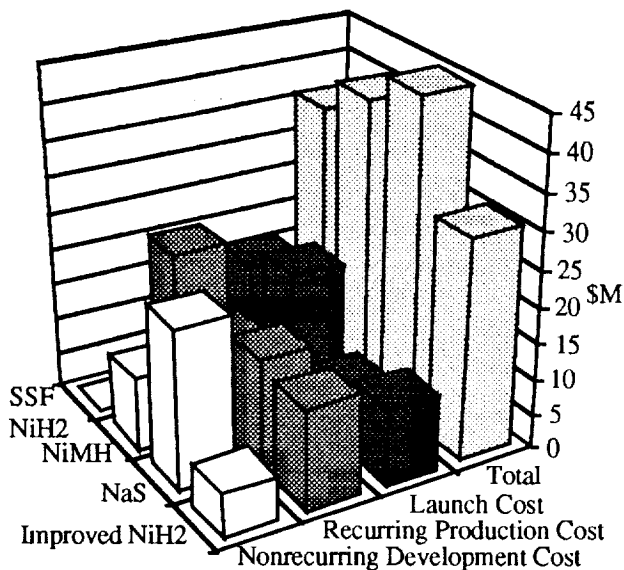


Figure 1 - Relative Cost of Batteries (75 kW)

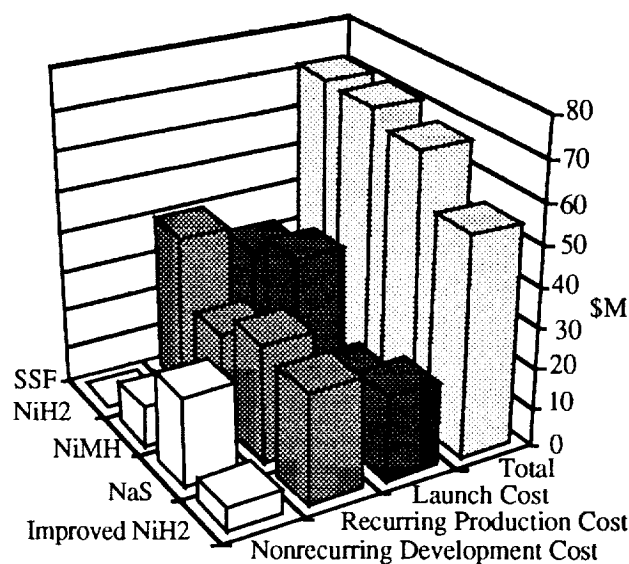


Figure 2 - Relative Cost of Batteries (150 kW)

Results showed that Improved NiH2 met the performance goal at the least cost for both 75 kW and 150 kW battery complements. At the 75 kW level, baseline NiH2 came in second to Improved NiH2. NiMH and NaS were both more costly. In the 150 kW analysis, NaS came in second to Improved NiH2. This was primarily because low NaS weight resulted in reduced launch cost. Over the 30 year life of SSF, a five year battery life would require launching as many as five replacement sets of 150 kW battery complements. Low NaS weight resulted in comparable savings to Improved NiH2 toward the end of this period.

Analysis showed that Improved NiH2 technology offers the best performance for the cost of battery technologies considered. Improved NiH2 batteries should be developed for SSF growth and for initial battery replacement at the end of their design life. NaS batteries show promise for savings towards the end of SSF design life. An investigation should be undertaken to establish the NaS depth of discharge versus cycle life relationship. Once this has been established, a better assessment between NaS and Improved NiH2 technologies can be made.

### **3.4 Roadmap Analysis**

Roadmaps were generated for promising battery technologies to describe the development required to achieve readiness level 6 (engineering model tested in relevant environment). In emerging technologies this process is speculative. The roadmaps include our assessment of all tasks required to mature each technology, some of which are already underway. At a readiness level 6 milestone, if a decision to incorporate that technology into a real program were made, that technology would follow a Phase C/D development process to launch. A conservative value of six years was estimated for this process (ref. 1).

Roadmaps for Improved NiH2 and NaS battery technology were generated from historical battery technology roadmaps tailored for specific development issues and tasks. ROM costs of each phase of development were also predicted. Launch of flight hardware was shown no sooner than five years after battery readiness level 6 was achieved. This five year period was provided to allow battery level real-time mission simulation to confirm capability. Confirmation is required because of the complex interaction of battery cell design, thermal design, charge control, and applied charge/discharge rates on mission life and performance.

Technology roadmap for Improved NiH2 appears in Figure 3. A key issue to be resolved is the isolation of charged active material on discharge by a nonconducting discharge crystal phase form. Testing of 26% aqueous potassium hydroxide electrolyte, sponsored by NASA LeRC, has demonstrated significant cycle life improvement at higher DoD's by limiting isolation of active material at the prototype cell level. Improving conductivity through the discharge crystal phase form by additives and limiting corrosion of the nickel current collector may also limit charged active material isolation. At the battery level, charge control and thermal management are critical to the formation of the bimodal charged crystal phase mix. Precision of charge control in flight batteries is critical to reducing battery stress and prolonging battery life. Implementation of charge control via hydrogen pressure may limit overcharge, limit charge material isolation, and offer improved autonomy as a state of charge indicator. Reduction of current density at the nickel electrode, improved oxygen gas management, and improved manufacturing quality may improve the DoD versus cycle life relationship. Developments proven at the component, cell, and battery levels will be integrated into a real-time model cell cycle life test to prove 30,000 cycle (5 year ) capability. Later a similar real-time battery test under simulated flight conditions would be undertaken.

A similar technology roadmap for tubular electrolyte NaS was prepared. Demonstration of the intrinsic capability of the cell design to perform for the LEO high cycle requirement has priority. The issues of micro-crack formation and cantilever suspension design of the alumina solid electrolyte need to be examined. Micro-gravity effects on cell operation, corrosion of cell seals, and accelerated corrosion beyond 60% DoD are also issues. Elements of battery charge control have to be established. Methods of operational cell balancing and cell open-circuit bypass hardware may be needed. NaS battery thermal management requires new approaches such as high temperature heat pipes or louver thermal windows, new thermal blanket technology, and cold launch scenarios.

### **3.5 Battery Conclusions**

Improved NiH2 offers the most attractive cost benefit analysis results, least technical risk, and least potential impact to SSF. It is recommended that the development of Improved NiH2 proceed for the SSF growth and upgrade application. Tubular electrolyte NaS has the advantage of low material cost and very high name plate specific energy resulting in potentially low weight. This may result in cost savings for the SSF application towards the end of its

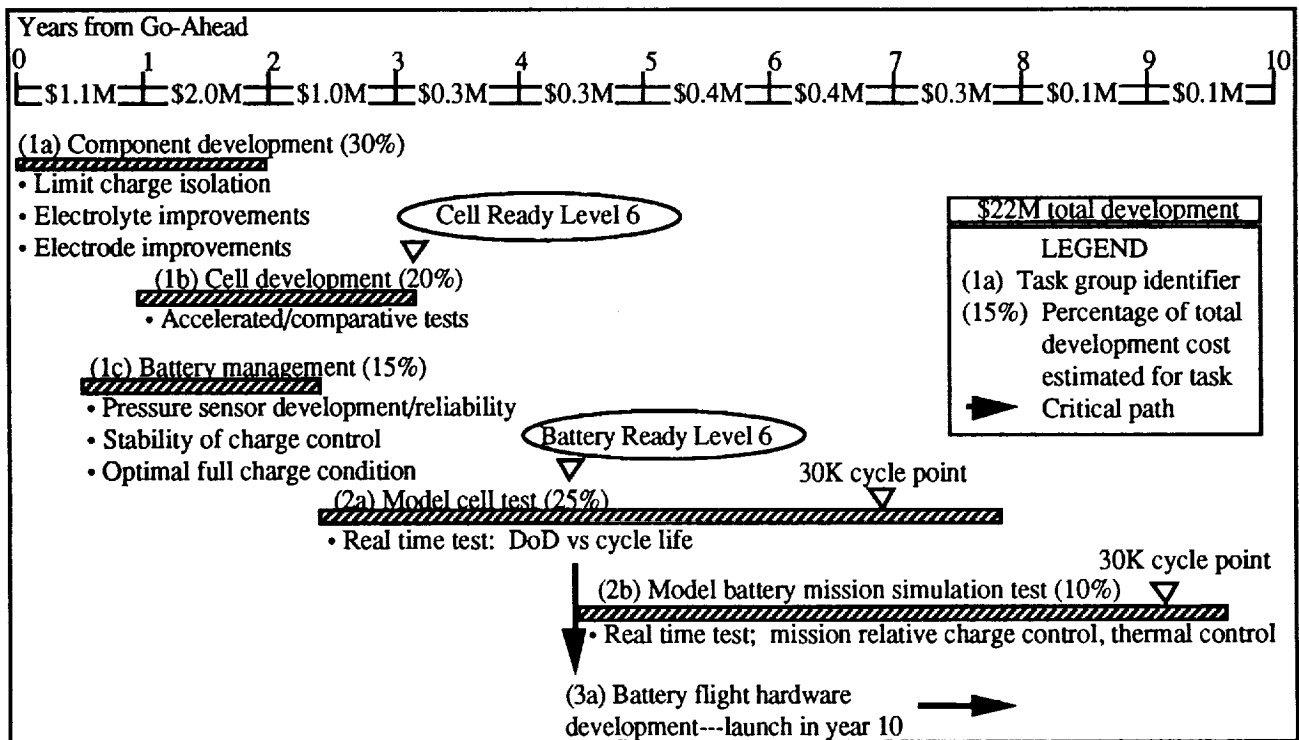


Figure 3 - Improved NiH2 Battery Roadmap

design life. It is recommended that the intrinsic NaS cycle life be established to determine the operational specific energy and actual weight savings. NaS battery and thermal management investigations should not proceed until intrinsic cell cycle life has been demonstrated.

#### 4.0 Advanced Photovoltaics

##### 4.1 Technical Readiness Assessment

Technical readiness of the 32 solar cell/array designs evaluated in this study is shown in Table III. The assessment was based on technology maturity and capability of large scale production startup in 1996-1997. Array technology was either based on the present SSF solar array design (ref. 8) (adapted to a study baseline planar array) or one of three concentrator array designs; General Dynamics Solar Low Aperture Troughs (SLATS), TRW Mini-Cassegrainian (ref. 9), or Boeing Minidome (ref. 10). The study baseline planar array design was used to simplify cell-to-cell comparisons and minimize development cost of new planar array structure. The technology performance goal was to double the SSF array areal power of 95 W/sq m while maintaining a power density over 80 W/kg. Areal performance was viewed as most critical due to array contribution to SSF atmospheric drag. Estimates of NASA readiness and risk level (defined in 3.1) were assigned on the basis of flight experience, cell production, and published papers.

**Planar Array Technology.** To compare planar solar cells, on-orbit expected BOL efficiencies were computed for each cell from its specified standard condition electrical efficiency and the expected panel operating temperature. Projected efficiencies for immature cell designs were derated to reduce risk. Array BOL areal power for the comparison cells were given by the ratio of the comparison cell efficiency over the baseline 8 mil Si cell efficiency multiplied by the SSF array areal power, 95 W/sq m (ref. 8). The BOL cell efficiencies and resulting areal powers are shown in Table III. By using this ratio method, common array design factors such as harness loss and tracking error were included.

**Concentrator Array Technology.** Data for SLATS and Mini-Cassegrainian, taken from the literature, and Minidome, taken from Boeing, indicated these arrays exceeded the performance goal. The concentrator designs all used a GaAs/GaSb tandem cell or equivalent (31% efficient at 100 AMO, 25°C).

Table III - Advanced Photovoltaics Technology Assessment

System Concept	Cell BOL % Efficiency	BOL Perf W/kg, W/sqm*	Readiness Level	Risk Level	System Concept	Cell BOL % Efficiency	BOL Perf W/kg, W/sqm*	Readiness Level	Risk Level
<b>SOA</b>					• CLEFT AlGaAs/CIS Tandem	26.0	85, 179	4	5
• Si WTC 8mil (SSF)	14.6	43, 95	7	1	• AlGaAs/active Ge	25.0	81, 170	4	5
<b>Advanced</b>					• AlGaAs/Si Tandem	32.0	111, 222	2	7
• "K7" Si, 2 mil	13.5	46, 87	7	2	• AlGaAs/InGaAsP	32.0	100, 220	2	7
• GaAs/inactive Ge, 3.5 mil	20.0	56, 135	5	3	• AlGaAs/active GaAs	24.0	59, 169	3	6
• AlGaAs/inactive GaAs	16.0	38, 108	3	5	• Epitaxial GaAs/Si	21.0	77, 146	2	6
• GaAs/Ge WTC, 7 mil	16.0	44, 135	5	4	• InAlAs/GaAs	26.0	64, 177	2	6
• GaAs/Ge IDC, 3.5 mil	16.0	56, 135	5	4	• GaInP2 Top Cell/Si	30.3	98, 212	3	6
• InP	20.0	49, 131	6	4	• GaInAs&GaInAsP Bottom Cell	25.0	82, 172	3	6
• GaAs/Ge, 7 mil	16.0	44, 135	6	2	• Amorphous Si	13.0	49, 86	3	5
• CLEFT GaAs/CIS	21.0	67, 142	6	4	• AlGaAs/GaAs/InGaAs	26.0	64, 177	3	6
• GaAs/GaSb SLATS	31.0	66, 200	6	5	• AlGaAs/GaAs/InGaAsP	26.0	64, 177	3	6
• GaAs/GaSb Minidome	31.0	100, 300	6	5	• InP/GaInAs Concentrator	28.0	94, 230	3	6
• APSA	13.5	100, 117	6	3	• GaAs/GaSb Mini-Cassegrainian	31.0	82, 257	6	5
• Silicon PERL	20.8	69, 135	4	6	• GaAs/GaInAs(P)/inactive Ge	25.0	81, 170	4	5
• Front Contact PIN Si	21.0	72, 141	4	6	• GaInP2/GaAs/inactive Ge	25.0	81, 170	4	5
• CLEFT InP	20.0	68, 135	2	7					
• CLEFT GaAs	21.0	73, 146	6	4					

\* Blanket-level performance estimates. Planar arrays assume use of modified SSF array structure. Each concentrator uses unique array structure.

## 4.2 Screening Results

The key screening criteria was performance. Areal powers in Table III were divided into three groups. The first group included most of the single junction cells with performance near 140-150 W/sq m. The second group at 170-180 W/sq m included most of the mature multijunction and tandem cells. The last group, over 200 W/sq m, included concentrators and advanced multijunction and tandem cells. With the increased array packing factor discussed above, performance of the three groups shifted to 160-179, 195-205, and over 220. The second and third groups then passed the performance goal. Other screening criteria were producibility cost and ease of array fabrication.

**Planar Array Technology.** Four planar cells were selected for further analysis; CLEFT AlGaAs/CIS tandem, AlGaAs/Si tandem, AlGaAs/active Ge multijunction (or variants GaAs/GaInAs/inactive Ge, GaAs/GaInAsP/inactive Ge), and GaInP2/GaAs/inactive Ge multijunction. These cells offered promising performance versus risk. Other cells may also be suitable but should not be substantially different than these.

**Concentrator Array Technology.** The Minidome and SLATS concentrators were selected for further analysis. A high SSF contamination environment was a concern for EOL array performance, especially for the SLATS and Mini-Cassegrainian designs. The baseline SSF planar array has a 15% contamination loss factor after 15 years. With a planar array or the Minidome design, light makes only one pass through the contamination layer. SLATS requires incoming light to pass through the contamination layer three times (in and out of one optical surface and then into cell). Mini-Cassegrainian requires the incoming light to pass through the contamination layer five times (in and out of two optical surfaces and then into cell). These designs may require more than a 15% contamination loss factor.

Mini-Cassegrainian was eliminated because of this potentially large contamination loss and its optical complexity. The design should not be completely eliminated from consideration until it is shown that contamination is a problem.

### 4.3 Cost/Benefit Analysis

Relative array costs over a 15 year period were computed for the screened array designs. Only costs that discriminated between technologies were estimated. These costs consisted of technology development, hardware production, launch, and reboost (\$/sq m drag area). Reboost cost is the cost of launching propellant to SSF to reboost it back to a higher orbit to make up for atmospheric drag.

In order to proceed to a cost estimate, a total array size had to be estimated for each candidate. It was determined that 75 kW of useable power required a 218 kW array based on the following factors; 0.80 battery charge efficiency, 42 minute full charge, 36 minute eclipse, and the following loss factors: 0.98 UV, 0.95 thermal cycle, 0.85 contamination, 0.98 meteoroid/debris, and 0.92 radiation. Since radiation degradation of the selected cell types was expected to be lower than the baseline Si but was unknown for most of the cells, a constant 8% radiation loss was assumed for all arrays. The 8% radiation loss was a simplification that favored the baseline Si array but was probably over-conservative for the concentrators. Another change to reduce planar array area was to increase the packing factor to 79% from the SSF array value of approximately 69% (ref. 8). This was accomplished by filling in empty panels (2%), eliminating the space where transverse panel longerons used to be (3%), and decreasing interpanel hinge spacing (5%). Resulting array areas and masses were calculated.

Estimated cell and array fabrication costs are shown in Table IV. Three specific cell costs were used as a cell point of departure: GaAs/GaSb estimate, GaAs/inactive Ge estimate, and baseline SSF Si cost (ref. 1). The cost of the other advanced cells were scaled from these. SSF array costs were used as an array point of departure. Total cost of the SSF arrays was given as approximately \$400,000,000, half non-recurring and half recurring, for 246.4 kW (75 kW useable power from four PV power modules) (ref. 1). In Table IV, the cost of baseline SSF Si arrays for the second 75 kW (for a total of 150 kW) was just the recurring cost stated above. The cost for advanced planar arrays was the

Table IV - Relative Fabrication Cost of Solar Arrays for SSF Upgrade/Growth

<b>CELL COSTS (DOLLARS)</b>							
Start with ~\$300/5.5 X 6 cm GaAs/inactive Ge cell, ~10,000 cells.							
Scale up to 8 x 8 cm (x1.93), very large quantities (x0.86), yields \$500/8 x 8 cell.							
Now add complexity factors for other cells compared to GaAs/Ge:							
Cell Type	Factor	Rationale			Cell Cost (8x8 cm equiv cell area)		
AlGaAs/Silicon	1.75	Two cells, somewhat fragile silicon substrate			\$875		
AlGaAs/CIS	1.5	Two cells, CIS is rugged			\$750		
AlGaAs/Ge	1.1	Almost the same as GaAs/inactive Ge			\$550		
GaAs/GaSb mini	0.54	Small, complex cells, 1/50 the area of planar			\$269		
GaAs/GaSb SLATS	0.75	Small, complex cells, 1/20 the area of planar			\$375		
Baseline Silicon	0.35				\$175		
<b>ARRAY COSTS (\$ MILLIONS)</b>							
Cell Type	Nonrecurring Cell Costs	Recurring Cell Costs	Labor Costs	Structure		Test	Total Fabrication
				Non-Recurring	Recurring		
AlGaAs/Silicon	\$20	\$138	\$52	\$5	\$28	\$19	\$262
AlGaAs/CIS	\$20	\$124	\$54	\$5	\$29	\$19	\$251
AlGaAs/Ge	\$20	\$95	\$57	\$5	\$30	\$19	\$226
GaAs/GaSb mini	\$8	\$30	\$94	\$45	\$50	\$35	\$262
GaAs/GaSb SLATS	\$11	\$58	\$88	\$35	\$47	\$33	\$272
Baseline Silicon	\$0	\$50	\$91	\$0	\$49	\$10	\$200

sum of modifying the existing SSF array to accept new cells plus recurring costs. Minidome and SLATS concentrator array costs included the total cost of cells and structure, assuming no benefit from SSF array development because of the large differences between concentrator and planar arrays. This assumption may have over-penalized the concentrators. Minidome costs were based on estimates from the Boeing array developers. SLATS costs were scaled from Minidome costs. Advanced array fabrication costs were all comparable in Table IV.

Launch and reboost costs were based on a Space Shuttle launch cost factor of \$4620/kg, and a SSF reboost cost factor of \$26,900 per drag square meter per year (ref. 1). Other costs such as EVA activity were assumed to be the same for all array types and were not included. Figure 4 indicates that relative array costs for all advanced arrays were much lower than the baseline array, primarily because of reduced reboost costs. In order to reduce anticipated high reboost costs, we assumed that arrays would be feathered during eclipse to reduce drag, an option that is not presently planned for SSF. If the present SSF no-feathering operational scenario had been assumed, reboost costs would have been approximately 40% higher than shown. Figure 4 shows that the Minidome concentrator had the lowest relative cost, followed closely by the planar arrays. The winning arrays were all about equal in cost when uncertainties in the estimates were considered.

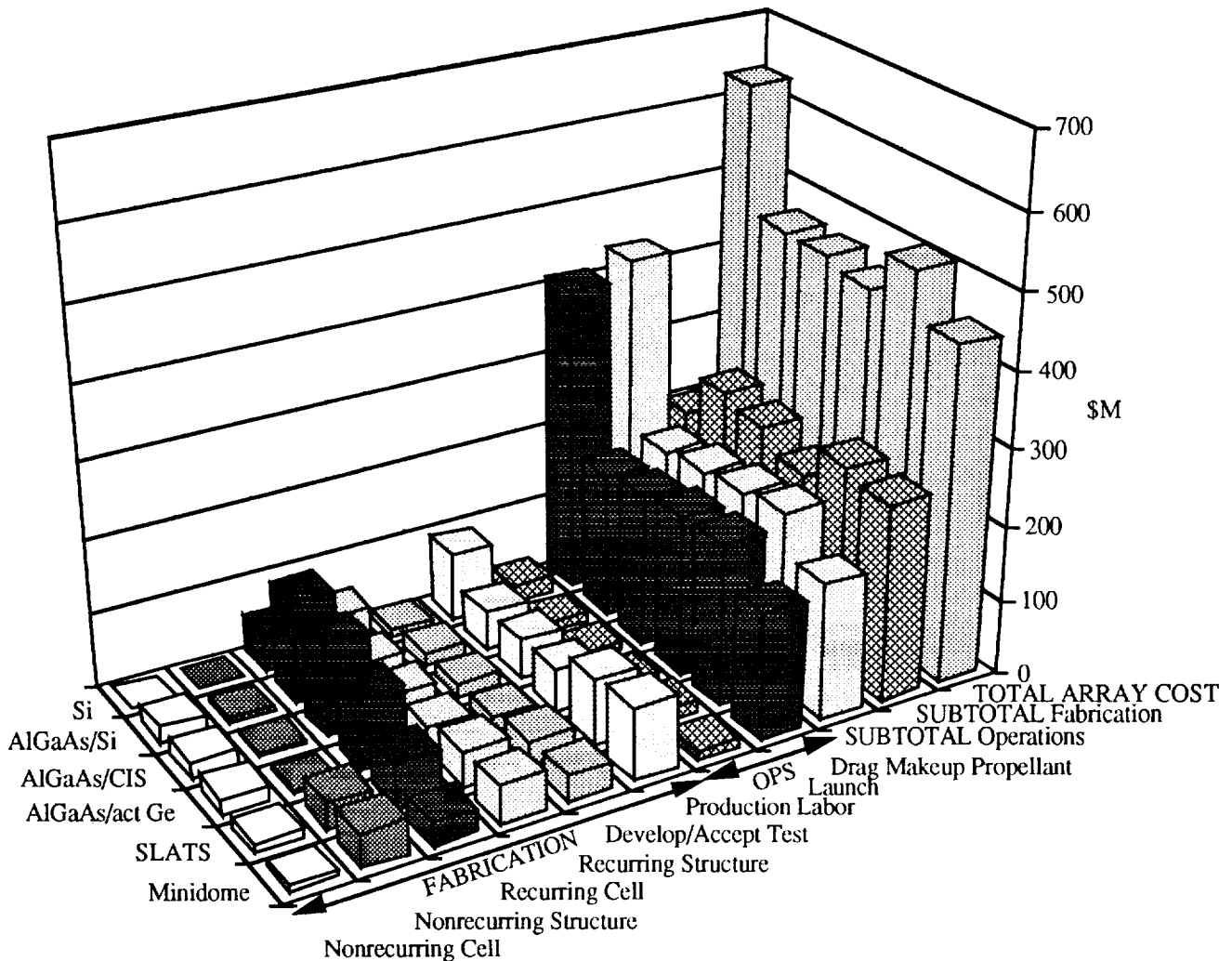


Figure 4 - Relative Cost of Solar Arrays for SSF Upgrade/Growth



#### 4.4 Roadmap Analysis

Roadmaps were generated for selected advanced arrays in the same manner as that described for batteries above. We identified initial technology development steps that were similar for all advanced planar arrays considered. The steps include: development of electrical efficiency and cell process in small cells, increase in cell size while controlling cost, and modification of existing array blankets and circuitry to accept new cell types.

A key development issue that applies to all advanced arrays in a SSF application is the determination of an accurate contamination loss factor. Front surface concentrator optics are especially vulnerable to contamination, and multijunction cells may also be at risk. Series interconnection makes multijunction cells susceptible to current limiting losses beyond the normal 15% if the contamination is spectrally selective. It is possible that contamination will cause one or more of the selected array concepts to drop out before an initial development effort is undertaken.

Minidome technology development roadmap is shown in Figure 5. Other roadmaps for SLATS, tandem cell (AlGaAs/CIS or AlGaAs/Si), and multijunction cell (AlGaAs/active Ge, GaInP2/GaAs/ inactive Ge, or GaAs/GaInAs(P)/ inactive Ge) arrays were prepared. Both SLATS and Minidome will need structure development. Concentrator pointing requirements must be accounted for with possible design impacts in the joints and main structure. Initial cell development and module demonstration for Minidome have been accomplished. Finalization of optics design with regard to cost and pointing requirements is continuing. Latest optical designs allow for an increase in pointing tolerance from 3° to 4°, but there will still probably be design impacts on the present SSF tracking mechanisms.

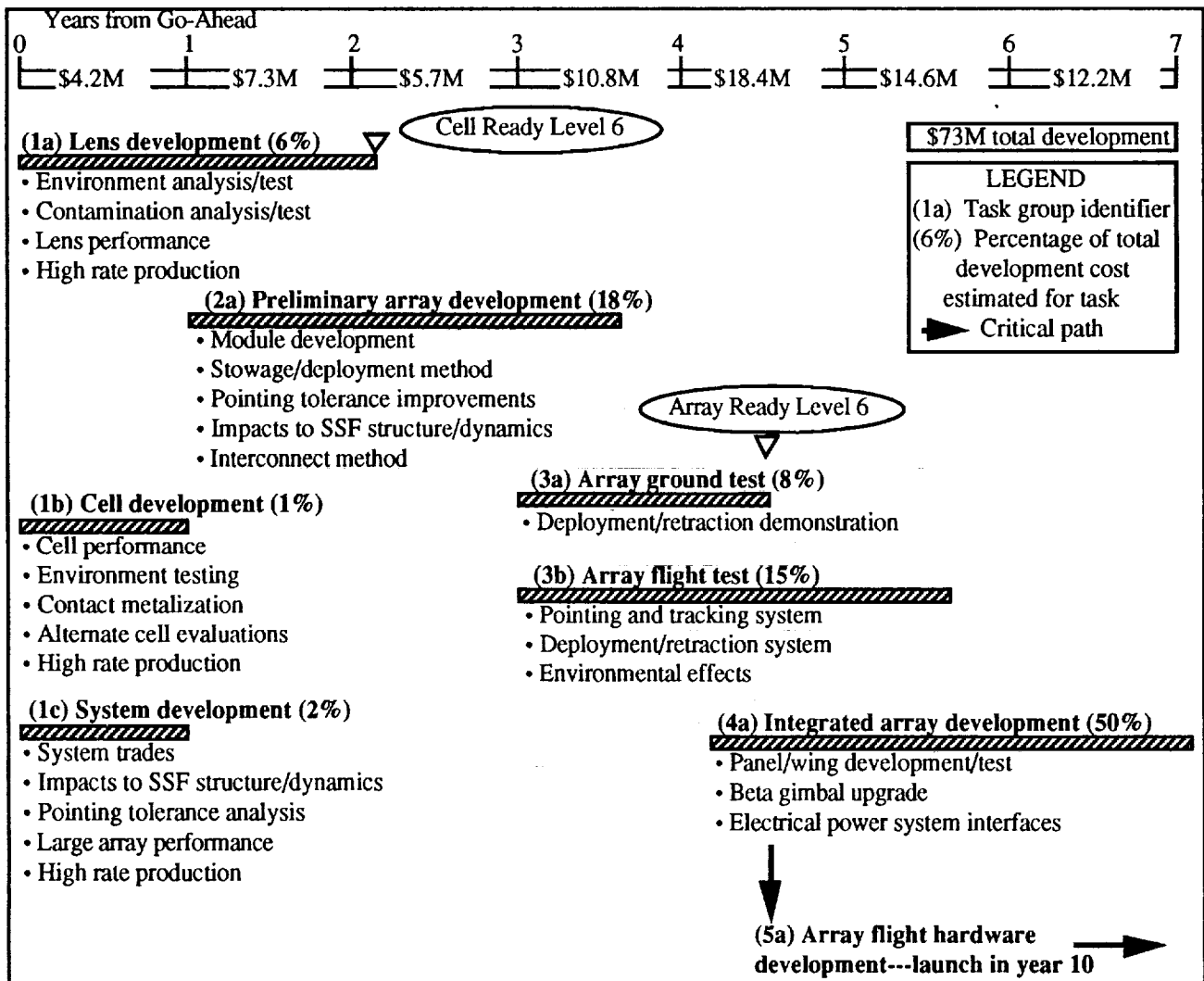


Figure 5 - Minidome Concentrator Array Roadmap

The SLATS concentrator array has been developed in a threat hardened form for the 10 kW Survivable Power Subsystem Demonstration (SUPER) array effort. It was assumed that this design was relatively mature for a concentrator and that much of the development could be used for a SSF application. If this is not valid, larger development costs would result. Contamination may be a problem, and the effect of the meteoroid/debris environment on optical efficiency needs to be determined.

#### **4.5 PV Conclusions**

This study identified several promising advanced PV concepts for SSF growth or upgrade. The concepts are only moderately complex and offer significant performance improvements and substantial cost savings. It is recommended that an early assessment of the expected SSF contamination environment and its impact on these technologies be undertaken. In parallel, initial development tasks should be performed for Minidome and SLATS concentrator arrays, and tandem cell (AlGaAs/CIS or AlGaAs/Si) and multijunction cell (AlGaAs/active Ge, GaInP2/GaAs/inactive Ge, or GaAs/GaInAs(P)/inactive Ge) arrays. After these initial tasks are accomplished, more accurate estimates of future array performance for SSF application can be made. Downselection to the most promising technology could then be accomplished.

#### **5.0 Study Conclusions**

Roadmaps generated for the most promising advanced battery and PV technologies provide focused development toward SSF growth, SSF upgrade, and LEO space platform applications. Funding of technology development steps described in these roadmaps, and resolution of associated development issues, will accelerate technology readiness and give hardware programs earlier access to cost effective advanced technologies for their application.

#### **6.0 References**

1. Cox, S.M., Gates, M.T., Verzwylt, S.A., Advanced SSF High Efficiency Power Systems Technology Development Planning, Boeing Defense & Space Group, D567-32000-1, March 31, 1992
2. Frate, D.T., Nickel-Hydrogen Cell Low-Earth-Orbit Life Test Update, 1991 IECEC Proceedings, Vol. 3, pp 263-266.
3. Hill, C.H., Matsumoto, J.M., Poston, T.M., Prater, A., Brown, H., Hall, S., and House, S., Air Force Nickel Hydrogen Cell Low Earth Orbit Life Test-Update, 1992 IECEC Proceedings, Vol. 1, pp.131-139.
4. Lim, H.S., Verzwylt, S.A., KOH Concentration Effect on the Cycle Life of Nickel-Hydrogen Cells, III. Cycle Life Test, Journal of Power Sources, 1988, Vol. 22, pp. 213-220.
5. Smithrick J.J. and Hall, S., Validation Test of Advanced Technology for IPV Nickel-Hydrogen Flight Cells - Update, 1992 IECEC Proceedings, Vol. 1, pp. 215-225.
6. Otzinger, B., Accelerated Cycle Life Performance for Ovonic Nickel-Metal Hydride Cells, 1990 NASA Aerospace Battery Workshop, pp. 547-557.
7. Sernka, R.P., Sodium-Sulfur- An Advanced Battery for Space, IAAA/DARPA Meeting on Light Weight Satellite Systems, 1987, p35-38.
8. Barona, C., Status of the SSF Solar Array, Space Photovoltaic Research and Technology Conference, Lewis Research Center, Nov 9,1989.
9. Solar Concentrator Array Development Final Technical Report, NASA 37439, Sept 30,1991.
10. O'Neill, M.J., Piszczor, M.F., Fraas, L.M., Key Results of the Mini-Dome Fresnel Lens Concentrator Array Development Program Under Recently Completed NASA & SDIO SBIR Reports, Space Photovoltaic Research and Technology Conference, 1991, pp 20-1 to 20-12.